DMD Fast Forward. Published on April 19, 2007 as doi:10.1124/dmd.106.014449

DMD #14449

METABOLISM AND DISPOSITION OF A SELECTIVE α_7 NICOTINIC ACETYLCHOLINE RECEPTOR AGONIST IN HUMANS

Christopher L. Shaffer, Mithat Gunduz[1], Renato J. Scialis and Annie F. Fang

Departments of Pharmacokinetics, Pharmacodynamics and Metabolism (C.L.S., M.G., R.J.S.) and Clinical Pharmacology (A.F.F.), Pfizer Global Research and Development, Groton/New London and Kalamazoo Laboratories, Pfizer Inc., USA

DMD Fast Forward. Published on April 19, 2007 as DOI: 10.1124/dmd.106.014449
This article has not been copyedited and formatted. The final version may differ from this version.

Running Title: Human Metabolism and Disposition of an α_7 nAChR Agonist

Address correspondence to:

Dr. Christopher L. Shaffer
Pharmacokinetics, Dynamics and Metabolism
Pfizer Global Research and Development
Groton/New London Laboratories
Pfizer Inc.
Eastern Point Road, MS 8220–4186
Groton, CT 06340
Tel. 860.441.3377
Fax 860.686.6532
Email: Christopher.L.Shaffer@pfizer.com

Text pages: 30
Tables: 5
Figures: 4
References: 24
Words in Abstract: 250
Words in Introduction: 308
Words in Discussion: 1,487

Abbreviations: 1, *N*-(3*R*)-1-azabicyclo[2.2.2]oct-3-ylfuro[2,3-*c*]pyridine-5-carboxamide (2*E*)-2-butanedioate; [^{3}H]**1**, 7-tritio-*N*-(3*R*)-1-azabicyclo[2.2.2]oct-3-ylfuro[2,3-*c*]pyridine-5-carboxamide ditrifluoroacetate; **2**, *N*-(3*R*)-1-azabicyclo[2.2.2]oct-3-ylcarbamoyl-5-hydroxypyridin-4-yl-acetic acid; **4**, *N*-(3*R*)-1-azabicyclo[2.2.2]oct-3-ylfuro[2,3-*c*]pyridine-5-carboxamide-1-*N*-oxide; CYP(s), cytochrome(s) P450; FMO, FAD-containing monooxygenase; HTO, tritiated water; LSC, liquid scintillation counting; LC-MS/MS, liquid chromatography-tandem mass spectrometry; HPLC, high performance liquid chromatography; AUC, area under the plasma concentration-time curve; k_{el}, elimination rate constant; LLOQ, lower limit of quantification; rcf, relative centrifugal force; MRM, multiple-reaction monitoring; HLM(s), human liver microsome(s); HKM(s), human kidney microsome(s); NADPH, reduced β-nicotinamide adenine dinucleotide phosphate; LC t_R, liquid chromatography retention time; CID, collision-induced dissociation.

Abstract

The metabolism and disposition of *N*-(3*R*)-1-azabicyclo[2.2.2]oct-3-ylfuro[2,3-*c*]pyridine-5-carboxamide (**1**), an α_7 nicotinic acetylcholinergic receptor agonist, were elucidated in humans (4 female, 4 male; all Caucasian) following an oral dose of [^{3}H]**1**. Overall, **1** was well tolerated, with >94% of administered radioactivity excreted renally by 48 h post-dose; lyophilization of all urine and plasma samples confirmed ^{3}H-stability within [^{3}H]**1**. Across genders, **1** underwent low-to-moderate oral clearance comprised of both renal (67%) and metabolic (33%) components, with the biotransformation of **1** occurring predominately via oxidation of its furanopyridine moiety to carboxylic acid **2**, and minimally by modification of its quinuclidine nitrogen to *N*-oxide **4** or *N*-glucuronide **M5**. Experiments using human *in vitro* systems were undertaken to better understand the enzyme(s) involved in the Phase 1 biotransformation pathways. The formation of **2** was found to be mediated by CYP2D6, a polymorphically expressed enzyme absent in 5–10% of Caucasians, while the generation of **4** was catalyzed by CYP2D6, FMO1 and FMO3. Interestingly, although no overall gender-related differences in excretory routes, mass recoveries, pharmacokinetics or metabolite profiles of **1** were evident, the observation of one of eight subjects (13%) showing disparate (relative to all other volunteers) systemic exposures to **1**, and urinary and plasma quantitative profiles nearly devoid of **2** with highest levels of **1**, seem consistent with both the identification of CYP2D6 as the only major recombinant CYP transforming **1** to **2** and the demographics of Caucasian CYP2D6 poor metabolizers. Data also reported herein suggest that **4** is generated predominately by renal FMO1 in humans.

Introduction

Schizophrenia, a disease affecting approximately 1% of the population (Sawa and Snyder, 2002), is comprised of positive (e.g. hallucinations) and negative (e.g. autism) symptoms as well as cognitive deficits (Green and Braff, 2001; Holden, 2003). Although typical and atypical antipsychotics have been successful at alleviating many symptoms of schizophrenia, their impact on cognition is not sufficient to enable the majority of patients with schizophrenia to lead normal productive lives (Meltzer and McGurk, 1999). However, recent evidence suggests a link between the α_7 subtype of neuronal nicotinic acetylcholine receptors (nAChRs) and cognitive deficits in schizophrenics (Freedman et al., 1997; Court et al., 1999; Marutle et al., 2001). Both partial (e.g. GTS-21) (Stevens et al., 1998) and full (Hajos et al., 2005) agonists of the α_7 nAChR have shown positive results in rodent models of cognitive improvement, and GTS-21 has demonstrated statistically significant improvements in human cognitive function (Kitagawa et al., 2003; Olincy et al., 2006). Hence, the development of a selective α_7 nAChR agonist may afford effective treatment for this currently unmet medical need of neurocognitive deficits in schizophrenics (Green and Braff, 2001; Breier, 2005).

N-(3*R*)-1-Azabicyclo[2.2.2]oct-3-ylfuro[2,3-*c*]pyridine-5-carboxamide (**1**), a novel α_7 nAChR agonist, demonstrated *in vivo* efficacy in both auditory sensory gating and rat novel object recognition, a preclinical model of cognitive performance (Wishka et al., 2006). The study reported herein was undertaken to determine definitively the metabolic and excretory pathways of **1** in humans following a single oral dose of [^{3}H]**1** (Figure 1). Although prior work (Shaffer et al., 2006) demonstrated the *in vivo* chemical and metabolic stability of the tritium atom within [^{3}H]**1** in both rats and dogs, all

collected human urine and plasma were nonetheless subjected to lyophilization to confirm empirically the expected tritium inertness. Elucidation of the clearance routes, metabolites and pharmacokinetics of **1** in the clinic has provided deeper insight into its overall human disposition.

Materials and Methods

Chemicals and Reagents. Compounds **1** (Wishka et al., 2006), **2** and **3** were prepared by the Synthesis Group at Pfizer Global Research and Development (PGRD, Kalamazoo, MI); [^{3}H]**1**•2TFA (17 Ci/mmol, 100% radiochemical purity) was made (Maxwell et al., 2006) by the Radiochemical Synthesis Group at PGRD (Kalamazoo, MI). The full chemical characterization of **1** (Wishka et al., 2006), [^{3}H]**1** (Maxwell et al., 2006), and **2** and **4** (Shaffer et al., 2006) have been reported previously. Metabolite **M5** was isolated from monkey urine following administration of [^{3}H]**1**, fully characterized by both mass spectrometry and LC-NMR, and provided by PDM at PGRD (Kalamazoo, MI). The chemical purity of all synthetic compounds was >99%. HLMs (21.7 mg protein/mL, 0.30 nmol P450/mg protein) pooled from 53 individual donors, and FMO1 (5.0 mg protein/mL, 0.52 nmol enzyme/mg protein) and FMO3 (5.0 mg protein/mL, 1.0 nmol enzyme/mg protein) SUPERSOMES™ were purchased from BD Gentest (Woburn, MA). CYP2D6 BACULOSOMES® (8.5 mg protein/mL, 0.12 nmol P450/mg) were procured from PanVera Corporation (Madison, WI) and HKMs (10.0 mg protein/mL) were obtained from XenoTech, LLC (Lenexa, KS). Chemicals and solvents of reagent or HPLC grade were supplied by Aldrich Fine Chemical Co. (Milwaukee, WI), Fisher Scientific (Pittsburgh, PA) and the J. T. Baker Chemical Co. (Phillipsburg, NJ). TruCount liquid scintillation cocktail was purchased from IN/US Systems, Inc. (Tampa, FL). All excreta and plasma were collected gravimetrically and stored at –70 °C until analysis.

Dosing of Human Volunteers and Collection of Samples. The study was an open-label, single-dose study to investigate the absorption, metabolism and excretion of **1** in

humans. The study population was comprised of eight healthy adult Caucasian volunteers (4 females, 4 males); women were required to be of non-child bearing potential (i.e. surgically sterile or post-menopausal with absence of menses for 1 y before study start). Subject demographics are summarized in Table 1. The Institutional Review Board (IRB) approved the study protocol, consent documents and protocol amendments prior to drug shipment. The clinical investigator was required to keep the IRB informed of the progress of the study and occurrence of any serious and/or unanticipated events. After being informed of the design, purpose and potential risks of the study, written informed consent was required from each subject prior to their enrollment at the Pharmacia Clinic Research Unit (Kalamazoo, MI), where they were kept under continuous medical surveillance from 12 h pre-dose to 192 h post-dose. Subjects were required to fast 10 h before and 4 h after dosing. Each subject was administered 40 mg (163 μCi) of [^{3}H]**1** dissolved in flavored Pedialyte® (10 mL), which was swallowed directly from a dosing bottle, followed by H_2O (100 mL). To determine the precise amount of radioactivity ingested by each subject, the dosing solution contained within their respective dosing bottle was analyzed both before and after dose administration to determine the amount of residual radioactivity within the dosing bottle. The difference in the amount of radioactivity detected within the dosing bottle before and after dose administration corresponded to the amount of radioactivity ingested by the subject (Table 1), which was the basis for determining subject dose recovery.

From each subject, urine was collected pre-dose and from 0–4, 4–8, 8–12 and 12–24 h during Day 1, and in 24 h intervals from 24–192 h post-dose, while feces were collected pre-dose and as passed at 24 or 48 h intervals for eight days post-dose. Blood

samples sufficient to provide 5 mL of plasma were collected into potassium-EDTA Vacutainer® tubes via arm venipuncture pre-dose and at 0.25, 0.5, 0.75, 1, 1.5, 2, 2.5, 3, 4, 5, 6, 8, 10, 12, 16, 24 and 48 h post-dose for the pharmacokinetic evaluation of **1** and total radioactivity. Blood samples sufficient to provide 20 mL of plasma were collected similarly at 1.5, 3, 6, 12, 24 and 48 h post-dose for the profiling of metabolites of **1**. Control plasma was harvested from pre-dose blood samples.

Determination of Radioactivity within Urine and Plasma. The following procedure was undertaken to quantify both total radioactivity and HTO within each urine and plasma sample: a gravimetric aliquot (4 g urine, 0.5 g plasma) from each time point was transferred to a Pyrex® borosilicate glass tube (12 × 75 mm), and triplicate gravimetric aliquots (0.5 g urine, 0.1 g plasma) were mixed with liquid scintillant (7 mL) and counted for 3 min by a Wallac 1409DSA liquid scintillation counter (PerkinElmer Life and Analytical Sciences, Inc., Wellesley, MA). Subsequently, each glass tube containing the remaining sample (2.5 g urine, 0.3 g plasma) was capped with a Kimwipe (to retain any freeze dried material undergoing "bumping" during sample lyophilization) secured by a rubber band, frozen at –20 °C and lyophilized using a FreeZone 4.5 Benchtop Freeze Dry System (Labconco Corp., Kansas City, MO). Each lyophilized sample was reconstituted in H_2O (2.5 g for urine, 0.3 g for plasma) and vortex-mixed. Triplicate gravimetric aliquots (0.5 g urine, 0.1 g plasma) of the reconstituted sample were combined with TruCount scintillation cocktail (7 mL) and subjected to LSC for 3 min. Additionally, each Kimwipe was immersed in scintillation cocktail (7 mL) and analyzed for radioactivity via LSC, and the amount of radioactivity detected within the Kimwipe was added to that detected in the lyophilized sample. The difference in total

radioactivity within each sample without and with lyophilization was attributed to HTO. Scintillation counter data were automatically corrected for counting efficiency using an external standardization technique and an instrument-stored quench curve generated from a series of sealed quench standards.

Determination of Radioactivity within Feces. Fecal samples were homogenized with H_2O (ca. 20% w/w, feces/H_2O) using a Stomacher homogenizer. Duplicate gravimetric aliquots (0.4–0.7 g) of fecal homogenate were transferred into tared cones and pads, weighed, dried for a minimum of 24 h at ambient temperature and combusted by a Packard Instruments Model A0387 sample oxidizer (Packard BioScience, Co., Meriden, CT). Combustion efficiency using a ^3H standard was determined daily before the combustion of study samples, and the measured radioactivity content in feces was adjusted using daily combustion efficiency values. The resulting HTO was trapped in Monophase-S® (Perkin Elmer Life and Analytical Sciences, Boston, MA), mixed in Perma-Fluor-E scintillation fluid (Packard BioScience, Co., Meriden, CT) and quantified over 10 min in a Packard Instruments Model 2300 liquid scintillation counter (Packard BioScience, Co., Meriden, CT). All combustion-related scintillation counter data were corrected for counting efficiency as explained previously.

Quantitative Analysis of 1 in Plasma. Plasma concentrations of **1** for each subject were determined using a validated LC-MS/MS assay at BASi (W. Lafayette, IN). Briefly, following the addition of an internal standard, individual plasma samples were loaded onto a 25 mg Isolute HCX-5 (C_4/SCX) plate, and sequentially washed with 50 mM ammonium acetate, 1 M acetic acid and MeOH. Analytes were eluted with 5% ammonium hydroxide in MeOH, evaporated to dryness and reconstituted in ammonium

DMD Fast Forward. Published on April 19, 2007 as DOI: 10.1124/dmd.106.014449
This article has not been copyedited and formatted. The final version may differ from this version.

acetate/MeCN mobile phase. Analytes within sample aliquots (150 µL) were eluted on a Phenomenex Synergi™ Polar-RP analytical column with an ammonium acetate/MeCN mobile phase. Instrument settings and potentials were adjusted to provide optimal data. Mass spectral data were collected using positive ionization in MRM scanning mode monitoring *m/z* 271.9→110.1 fragmentation for **1** (LC t_R = 3.6 min). The dynamic range of the assay was 1 to 1,000 ng/mL for **1**.

Calculations. Pharmacokinetic parameters were calculated for each subject by non-compartmental analyses using WinNonlin Version 3.2 (Pharsight Corp., Mountain View, CA). Values used to determine the pharmacokinetic parameters of total radioactivity were calculated by converting the LSC-generated raw data to concentrations (ng-eq./mL) using the specific activity (1.1 mCi/mmol) of administered [^{3}H]**1**. The $AUC_{0-tlast}$ was calculated using the linear trapezoidal method, k_{el} was determined by linear regression of the log concentration versus time data during the last observable elimination phase, and half-life ($t_{1/2}$) was calculated as $0.693/k_{el}$. T_{last} was 48 h for **1** and 16 h for total radioactivity. Both maximal plasma concentration (C_{max}) and its time of occurrence (T_{max}) were taken directly from the concentration versus time data. Means and standard deviations were calculated when half or greater of the values exceeded the LLOQ for **1** (1.0 ng/mL) or total radioactivity (11.3 ng-eq./mL). A value of 0 was used when a measured value was below its LLOQ. For each subject, oral plasma clearance (CL_p/F) of **1** was calculated by dividing the dose by respective plasma AUC_{0-48}, and oral renal clearance (CL_R/F) of **1** was determined by dividing the amount of **1** excreted unchanged in urine over 48 h (Ae_{0-48}), as determined by the radioprofiling of pooled individual urine (see below), by its plasma AUC_{0-48}; both clearance values were then subject weight-

normalized to afford units of mL/min/kg. Enzyme kinetics were calculated by Microsoft Excel® using Solver function (non-linear fitting), and were verified by GraphPad Prism v4.00 (GraphPad Software, Inc., San Diego, CA).

Sample Preparation for Metabolite Profiling and Identification. At each step during the sample preparation of all biological matrices, total radioactivity levels were determined by LSC for recovery calculations. Following preparation, all samples were analyzed as described below by LC-MS/MS with radiometric detection. Pre-dose and blank samples served as controls for determining background radioactivity and endogenous, non-drug-related ions observed within respective matrices or their extracts by LC-MS/MS.

Urine. LSC analysis of both pre- and post-lyophilization urine samples for each time point from each subject found no significant difference (i.e. ±5%) in the amount of radioactivity contained within each sample suggesting that no significant amount of HTO was contained within this matrix. Therefore, non-lyophilized urine samples from each subject collected from 0–48 h post-dose representing >95% of total urine radioactivity were pooled proportional to the amount of urine in each sampling period for analysis by LC-MS/MS with radiometric detection. Pooled urine samples (13–30 mL) were concentrated by a N_2 stream at 37 °C, reconstituted in 10 mM ammonium formate, pH 3.4 (1.2 mL, Solvent A) and centrifuged (1,811 rcf for 5 min) to afford the analytical sample, which retained ≥90% of the radioactivity contained within the pooled sample prior to concentration.

Feces. Due to trivial amounts (≤2% of dose) of detected radioactivity, feces were not profiled.

Plasma. LSC analysis of both pre- and post-lyophilization plasma samples for each time point from each subject found no significant difference (i.e. ±5%) in the amount of radioactivity contained within each sample suggesting that no appreciable amount of HTO was in any plasma sample. Thus, for each subject, non-lyophilized plasma from blood samples collected at 1.5, 3, 6 and 12 h post-dose were used for circulatory metabolite profiling and identification since ≥90% of the total radioactivity $AUC_{0–16}$ was captured by its $AUC_{0–12}$. Plasma samples were pooled according to the method of Hamilton *et al.* (Hamilton et al., 1981); i.e. 1.5, 2.25, 4.5 and 3.0 mL, respectively, of plasma from each time point were combined. This pooling procedure afforded one composite sample encompassing the entire AUC comprised by multiple individual time point samples allowing one sample injection to provide a representative of total exposures (AUC) to metabolites relative to each other. To remove dissolved proteins, pooled plasma samples (ca. 11.3 mL) were diluted with MeCN (23 mL), vortex-mixed for 10 min, centrifuged (2,465 rcf for 10 min) and the resulting supernatants, which contained >90% of the radioactivity from each pooled sample, were isolated. Each supernatant was concentrated to near dryness at 35 °C under N_2 and reconstituted in Solvent A (300 μL) to yield the analytical sample.

Metabolite Profiling and Identification. Samples were analyzed by an LC-MS/MS, comprised of a PE Sciex API-3000 tandem quadrupole mass spectrometer with a TurboIonSpray® interface (Perkin Elmer Life and Analytical Sciences, Boston, MA), two Shimadzu LC-10A HPLC pumps (Shimadzu USA, Columbia, MD) and a CTC PAL Autosampler (LEAP Technologies, Carrboro, NC), in series with a β-RAM radiometric detector (IN/US Systems, Inc.) containing a liquid scintillant cell (500 μL). Analytes

within sample aliquots (20–100 μL) were eluted on a Luna Phenyl-hexyl analytical column (5 μ, 4.6 × 250 mm; Phenomenex USA, Torrance, CA) at 1 mL/min with Solvent A and MeCN (Solvent B). The following two-step gradient was employed: 0–10 min, 2% solvent B in solvent A; 10–30 min, 2%–35% B in A; 30–32 min, 35%–90% B in A. Following the elution of **1** and its metabolites, the column was washed with 90% B in A for 3 min and then returned over 3 min to 2% B in A where it remained for 7 min prior to the next injection. For each matrix, >99% of the radioactivity injected onto the column eluted during the first 32 min of the gradient program. HPLC effluent was split 1:9 between the mass spectrometer and the radiometric flow detector; liquid scintillation cocktail flowed at 3 mL/min to the radiometric detector. Mass spectral data were collected using positive ionization in full, precursor ion, neutral loss, product ion and MRM scanning modes. Instrument settings and potentials were adjusted to provide optimal data in each mode. Analyst® 1.4 (Perkin Elmer Life and Analytical Sciences) and Winflow version 1.4 (IN/US Systems, Inc.) software were used for the acquisition and processing of mass spectral and radiochromatographic data, respectively.

Since the radioactivity in all reconstituted plasma samples was too low for quantification by radiometric flow detection, HPLC effluent was isolated in 30 s intervals by a Gilson FC 204 fraction collector (Gilson, Inc., Middleton, WI), and each respective fraction was mixed with scintillation fluid (7 mL) and subjected to LSC for 3 min. Individual plasma radiochromatograms were generated from respective liquid scintillation data using Microsoft Excel® (Microsoft Office 2000® 9.0.4402 SR-1) and paired with their respective MRM chromatograms.

***In Vitro* Incubations.** All *in vitro* incubation samples were analyzed by an LC-MS/MS system consisting of an API-4000™ tandem quadrupole mass spectrometer with an electrospray ionization source (Applied Biosystems, Foster City, CA), three Shimadzu LC-10ADvp binary pumps with DGU-14A Degasser (Shimadzu USA), CTC PAL Autosampler (LEAP Technologies) and a Valco EHMA Two Position Microelectric Valve Actuator (Valco Instruments Co. Inc., Houston, TX). Analytes within sample aliquots (10 μL) were eluted on a Phenomenex Synergi™ Max-RP analytical column (4 μ, 2.0 × 50 mm) at 0.25 mL/min with Solvent A and Solvent B using the following gradient: 0–2 min, 5% B in A (effluent diverted to waste); 2–4.5 min, 5%–35% B in A; 4.5–6 min, 35% B in A. Upon elution of **1**, **2** and **4**, the column was returned over 1 min to 5% B in A where it remained for 1 min before the next injection. Instrument settings and potentials were adjusted to provide optimal data. Mass spectral data were collected using positive ionization in MRM scanning mode monitoring *m/z* 271.7→110.3 (**1**, LC t_R = 4.3 min), *m/z* 306.0→110.2 (**2**, LC t_R = 3.6 min) and *m/z* 288.2→109.3 (**4**, LC t_R = 4.4 min). Quantification of **1**, **2** and **4** was accomplished using standard curves ranging from 1 to 10,000 nM. Analyst® 1.4.1 (Applied Biosystems, Foster City, CA) software was used for the acquisition and processing of mass spectral data.

Human Liver and Kidney Microsomes. HLM incubations (300 μL) were performed in duplicate with and without NADPH (0.3 μmol) in Thermo-Strips (ABgene, Epsom, UK) open to air at 37 °C on a Biomek® 2000 Laboratory Automation Workstation (Beckman Coulter, Inc., Fullerton, CA). Each incubation contained HLMs (0.8 mg protein/mL 0.1 M KH_2PO_4 buffer, pH 7.4) and **1** (1, 3, 10, 30, 100 or 300 pmol); total organic solvent content was <0.03% (v/v). Sample aliquots (45 μL) were removed

by micropipette at 0, 5, 15, 30, 45 and 60 min after NADPH (or buffer) addition, quenched with MeCN (255 μL) containing an internal standard and centrifuged (867 rcf for 15 min at 20 °C), and the resulting supernatant was analyzed by LC-MS/MS as described previously. Using the same incubation and analytical methodology as described for HLMs, HKM incubations (300 μL) were conducted similarly only differing in concentrations of protein and **1** (1.0 mg protein/mL and 300 pmol, respectively) and slightly different time points (i.e. 0, 5, 10, 15, 30 and 45 min after NADPH (or buffer) addition) for aliquot sampling.

CYP2D6 BACULOSOMES®. Incubations (300 μL) were performed in duplicate with and without NADPH (0.3 μmol) using the apparati employed for HLMs. Each incubation contained BACULOSOMES® expressing rCYP2D6 (0.4 mg protein/mL 0.1 M KH_2PO_4 buffer, pH 7.4) and **1** (0.03, 0.15, 0.3, 1.5, 3 or 15 nmol); total organic solvent content was <0.06% (v/v). For initial exploratory incubations (1 μM **1**), sample aliquots (45 μL) were removed by micropipette at 0, 5, 15, 30, 45 and 60 min after NADPH (or buffer) supplementation, and quenched and processed as described above to afford the analytical supernatant for LC-MS/MS analysis. These incubations demonstrated **1** was metabolized by CYP2D6, and both **2** (r^2=0.94) and **4** (r^2=0.96) were formed linearly from 0 to 45 min. Accordingly, subsequent incubations conducted to study enzyme kinetics had sample aliquots removed at 30 min after NADPH fortification.

Human FMO1 and FMO3 SUPERSOMES™. Incubations (300 μL) were performed in duplicate with and without NADPH (0.3 μmol) as described previously. Each incubation contained SUPERSOMES® expressing rFMO1 (0.1 mg protein/mL 0.1 M KH_2PO_4 buffer, pH 7.4) or rFMO3 (0.05 mg protein/mL buffer) and **1** (300 pmol).

Sample aliquots (45 μL) were removed by micropipette at 0, 5, 10, 15, 30 and 45 min after addition of **1** (or buffer), and quenched and processed as described above for LC-MS/MS analysis. FMO1 and FMO3 viability was confirmed by monitoring the NADPH-dependent conversion of the respective isozyme-selective substrates (both at 1 μM) imipramine (Lemoine et al., 1990) and benzydamine (Fisher et al., 2002) to their *N*-oxide metabolites.

Results

Clinical Observations. Eight volunteers (4 female, 4 male) were enrolled as planned, and all subjects completed the study and were evaluable for adverse events, safety laboratory tests and pharmacokinetics. There were no serious adverse events, withdrawals due to adverse events or deaths associated with this study. Following administration of **1**, three of eight subjects reported a total of five adverse events, the most common (60%) being nausea. There were no vital signs, electroencephalogram or safety laboratory test findings of potential clinical concern. Overall, **1** was well tolerated.

Excretion of Total Radioactivity. No readily apparent gender-related differences in overall excretory routes or mass recoveries were observed (Table 2). Lyophilization of all urine samples collected from each subject demonstrated that ≤2% of total urinary radioactivity was attributable to HTO. Mean overall recovery of excreted drug-derived material was 108%±6%, with essentially all radioactivity in urine (107%±6%) relative to feces (1.8%±0.3%). The excretion of total drug-related material was rapid in both genders; on average, >94% of administered radioactivity was excreted within the first 48 h post-dose. The recovery of radioactivity slightly greater than that dosed was investigated further by determining if light-dependent chemiluminescence within urine samples generated artificially high values outside of the standard deviation (i.e. ±5%) for control samples. However, LSC analysis of all urine samples after 48 h of storage in darkness generated identical dose recovery values, suggesting sample chemiluminescence was not occurring.

Pharmacokinetics of 1 and Total Radioactivity. Raw data for determining the pharmacokinetic parameters of **1** and total radioactivity were acquired using a validated

LC-MS/MS assay and LSC, respectively. Lyophilization of all plasma samples collected from each subject demonstrated that <1% of total circulatory radioactivity was attributable to HTO. In all subjects, quantifiable concentrations of **1** and total radioactivity were not detected within plasma sampled beyond 48 h and 16 h post-dose, respectively, defining these time points as respective T_{last} values. For **1** and total radioactivity, mean (±SD) male and female plasma concentrations vs. time are plotted in Figure 2, and mean (±SD) gender-differentiated pharmacokinetic parameters are listed in Table 3. Although all mean PK data for both **1** and total radioactivity were within 2-fold for both males and females, suggestive of no gender-related differences in the human disposition of **1**, females tended to have slightly higher systemic exposures of **1** (as measured by C_{max} and AUC) which corresponded to its longer half-lives and lower oral clearances, both total and renal (Table 3).

Structural Rationalization of 1 and Its Metabolites. Compound **1** had a protonated molecular ion of *m/z* 272 and an LC t_R of ca. 23.3 min. The CID product ion spectrum of *m/z* 272 contained fragment ions with *m/z* 163, 146, 118, 110 and 82 (Table 4). Precursor ion scanning of diagnostic fragment ions *m/z* 118 and 110 determined if metabolites of **1** were modified on its quinuclidine or furanopyridine moieties, respectively (Figure 1). A summary of all metabolite LC-MS/MS data is found in Table 4. The identification of a metabolite as a fully characterized standard was determined by the compounds' indistinguishable CID spectra and LC t_R, as well as an increase in metabolite MS peak height upon addition of the authentic standard to the analytical sample.

Quantitative Profile of [^{3}H]1 and Its Metabolites in Urine and Plasma. In addition to **1**, metabolites **2**, **4** and **M5** were observed in the urine of all subjects (Table

5). On average in females and males, 64.8%±13.7% and 71.5%±5.0% of administered **1**, respectively, was renally excreted. These data were in excellent agreement with the percentage of total oral clearance (CL_p/F) comprised by its renal component (CL_R/F) in both females (64.5%±13.3%) and males (70.8%±4.7%) (Table 3). In plasma, **1** and all urinary metabolites were also detected (Table 5). On average, **1** comprised 61.0%±16.4% and 57.0%±8.2% of total circulatory radioactivity in females and males, respectively, which were in good agreement with their respective pharmacokinetic-derived $AUC_{0–12}$ ratios for **1** and total radioactivity of 52.7%±13.2% and 46.1%±4.6%. Although no gender differences were observed in metabolite profiles qualitatively, one female subject (2F) had significantly different quantities of **1** and **2** in both urine (81.1% and 3.1%, respectively) and plasma (80.6% and 0.6%, respectively) relative to the other seven subjects (Table 5). On average, these subjects had 66.3%±9.4% and 28.6%±9.1% of dose attributable to **1** and **2** in urine, respectively, and 55.9%±9.2% and 26.1%±7.6% of total plasma ^3H comprised by **1** and **2**, respectively. This large quantitative difference in the metabolic profiles of subject 2F relative to other subjects is manifested in the much larger standard deviations for **1** and **2** in female urine and plasma than for those same matrices in male subjects (Table 5).

***In Vitro* Metabolism of 1.** Following identification of **2** as the major human metabolite of **1**, the possibility of the biotransformation of **1** to **2** being hepatically-mediated was studied in human-derived *in vitro* systems. In HLMs (0.8 mg protein/mL), no consumption of **1** (over a concentration range of 0.0032 to 1 μM) was observed regardless of NADPH. As a control, HLM viability was confirmed by its NADPH-dependent metabolism of atomoxetine (0.3 μM), which was fully consumed after 30 min.

Prior to the human radiolabeled metabolism study reported herein, preliminary *in vitro* reaction phenotyping experiments (unpublished Pfizer Inc. internal data) with individual cDNA-expressed major human CYPs (CYP1A1, CYP1A2, CYP2C9, CYP2C19, CYP2D6, CYP3A4 and CYP3A5) found only CYP2D6 to metabolize **1** (ca. 20% after 60 min of incubation). Therefore, following definitive elucidation of its human metabolic pathways, **1** was subjected to CYP2D6 BACULOSOMES® to determine if **2** was a CYP2D6-mediated metabolite. Initial exploratory incubations (1 μM **1**) confirmed **1** was metabolized by CYP2D6 to the same extent as previously reported (i.e. 20%), and found that **2** (r^2=0.94) and **4** (r^2=0.96) were formed linearly from 0 to 45 min. Subsequent incubations at various concentrations of **1** determined the enzyme kinetics of the CYP2D6-catalyzed oxidation of **1** to **2** (K_M = 5.0 μM) and **4** (K_M = 4.6 μM), which are found in Figure 3. Following CYP2D6 incubations, **1** (1 μM) was incubated with HKMs, FMO1 and FMO3 to explore the possibility of it being an FMO substrate. In each enzymatic system, **1** was exclusively converted to **4**, with its rate of generation occurring in the order of FMO1 (1.81 pmol **4**/min/mg) > FMO3 (0.204 pmol **4**/min/mg) > HKMs (0.0450 pmol **4**/min/mg).

DMD Fast Forward. Published on April 19, 2007 as DOI: 10.1124/dmd.106.014449
This article has not been copyedited and formatted. The final version may differ from this version.

Discussion

The metabolism and disposition of **1** was determined definitively in humans following a single dose of [^{3}H]**1** (40 mg, 163 μCi), which was well-tolerated in all eight healthy volunteers. Mean overall recovery of administered radioactivity, >94% of which was excreted within the first 48 h post-dose, was 108%±6%, with effectively all drug-derived material in urine (107%±6%). No significant difference in initial radioactivity detected within any urine or plasma sample following lyophilization confirmed the predicted *in vivo* ^{3}H-stability of [^{3}H]**1**, and demonstrates that judicious use of tritiated compounds can be effective in clinical mass balance studies. A combination across genders of short T_{max} and large amounts of urinary radioactivity excreted during the first 24 h post-dose suggested **1** was rapidly and substantially absorbed orally in humans. Across genders, **1** underwent low-to-moderate oral clearance comprised of both renal (ca. 67%) and metabolic (ca. 33%) components. Insignificant amounts (<2% of dose) of fecal radioactivity, coupled with the complete absorption of dose, suggest negligible (if any) biliary clearance of **1** in humans.

Essentially all ingested radioactivity was renally excreted, and the percent of total urinary dose attributable to **1** (Table 5) was equal to the contribution of renal clearance (CL_R/F) to systemic clearance (CL_p/F) (Table 3). Active renal secretion of **1** was observed as CL_R/F exceeded the glomerular filtration rate (GFR) of plasma-unbound **1** (Table 3). Although the data support the net renal secretion of **1** in humans, the full extent of this transporter-mediated process cannot currently be completely defined due to the possibility of concomitant active and/or passive renal reabsorption. The quinuclidine nitrogen (pK_a 9.0) within **1** dictates that at normal plasma or urine pH the vast majority

(≥98% per the Henderson-Hasselbach equation) of **1** will be protonated making it a likely substrate for one or more renal organic cation transporters.

Qualitatively identical and quantitatively similar metabolite profiles in all biological matrices across genders suggest no apparent sex-related differences in the overall metabolism of **1** in humans. A proposed schematic overview of the human metabolism of **1** is presented in Figure 4. Based on the identification of all urinary and circulatory metabolites, human biotransformation of **1** occurs predominately via oxidation of its furanopyridine moiety to **2**, and minimally by either monooxygenation or glucuronidation of its quinuclidine nitrogen to **4** or **M5**, respectively. In seven of eight subjects, **2** was the major metabolite, comprising ca. 21% of total circulatory radioactivity, possibly necessitating its future pharmacokinetic characterization in humans as a metabolite monitoring strategy (Baillie et al., 2002). All human metabolites, except **M5**, were observed previously (Shaffer et al., 2006) in rats and dogs confirming these as appropriate toxicological species. Although **M5** was not observed in these animals, its minor quantities (≤3%) and conjugative nature, indicative of a highly polar compound with a low volume of distribution and innocuous pharmacology, make it of little concern from a safety perspective (Smith and Obach, 2005).

Metabolism accounted for ca. 33% of the total human oral clearance of **1**, with the main biotransformation pathway (Table 5) of enzymological interest being the formation of **2** via furanopyridine oxidation of **1** (Figure 4). Prior to the human radiolabeled study described here, preliminary *in vitro* reaction phenotyping experiments (unpublished Pfizer Inc. internal data) with individual cDNA-expressed major human CYPs (CYP1A1, CYP1A2, CYP2C9, CYP2C19, CYP2D6, CYP3A4 and CYP3A5) and human FMOs

(FMO1 and FMO3) identified **1** as a substrate for CYP2D6 (ca. 20% consumption after 60 min) and FMO1 (ca. 40% consumption after 60 min) only. Following the human radiolabeled study and the identification of **2** as the major human metabolite of **1**, we revisited the human *in vitro* metabolism of **1** to further investigate this specific biotransformation pathway.

Initially, **1** was subjected to HLMs, but, irrespective of NADPH or substrate concentration, no turnover of **1** was observed, suggesting minimal (if any) contribution by liver microsomes to its human metabolic clearance. These microsomal incubations were conducted over a concentration range of **1** (0.0032 to 1.0 μM) at a fixed P450 concentration (0.25 μM), hence the lack of substrate consumption was not due to its enzyme saturation. An appropriate control substrate was used in all studies to confirm HLM viability, and secondary incubations were conducted to demonstrate no mechanism-based inactivation of HLMs by **1**. The lack of HLM oxidation of **1** precluded quantification of P450 isozyme-specific contributions to its human hepatic clearance. Next, using a recombinantly-expressed CYP2D6 system we also found that ca. 20% of **1** was consumed over 60 min. More importantly, this metabolism of **1** resulted in **2** and **4** (Figure 3). Subsequently, to determine the metabolites arising from the FMO-mediated biotransformation of **1**, it was subjected to recombinant human FMO1 and FMO3, as well as HKMs. Within each system, **1** was converted to **4** exclusively in an NADPH-dependent fashion occurring most rapidly with FMO1 (1.81 pmol **4**/min/mg protein) and most slowly in HKMs (0.0450 pmol **4**/min/mg protein). Due to the unknown amount of FMO within the employed HKMs, no rate comparisons may be made between the FMOs and HKMs. However, **4** formation rates may be compared directly for FMO1 and

FMO3, with the former generating **4** nine-times faster than the latter. In total, these *in vitro* studies suggested that in humans the biotransformation of **1** to **2** was most likely primarily CYP2D6-mediated, while the conversion of **1** to **4** could be undertaken by CYP2D6, FMO1 or FMO3.

The hepatic metabolic clearance (or lack thereof) in HLMs (CL_h <2.4 mL/min/kg) was much less than that observed in rat (RLMs; CL_h = 59 mL/min/kg) or dog (DLMs; CL_h = 21 mL/min/kg) liver microsomes (unpublished Pfizer Inc. internal data) as calculated by the well-stirred model incorporating all species-specific binding factors (i.e. microsomal free-fraction, plasma free-fraction and blood-to-plasma ratio) (Obach et al., 1997). Qualitative analyses of these preclinical incubations found the NADPH-dependent consumption of **1** corresponded to the simultaneous formation of **2** and **4** in RLMs, and **4** only in DLMs (unpublished Pfizer Inc. internal data). Although FMO1 is found in rat liver and in even higher abundances in dog liver, it is absent in human liver but present in human kidneys (Rettie and Fisher, 1999; Cashman, 2004). These species- and tissue-specific expression data are consistent with the conversion of **1** to **4** in rat and human kidney microsomes (with much greater amounts in rat tissue), recombinant human FMO1, RLMs and DLMs, but not in HLMs. Although **1** is converted to **4** (0.204 pmol **4**/min/mg protein) by recombinant FMO3, the predominately expressed FMO in human adult liver (Rettie and Fisher, 1999), this biotransformation was not observed in HLMs. This observation, supplemented by both the FMO1-mediated formation rate of **4** being nine-times faster than that of FMO3 and the greater quantity of **4** in urine versus plasma (Table 5) with no fecal elimination, strongly suggests, but does not prove, that **4** is generated by renal FMO1 in humans. These suspected FMO1-related *in vitro* data were

DMD Fast Forward. Published on April 19, 2007 as DOI: 10.1124/dmd.106.014449
This article has not been copyedited and formatted. The final version may differ from this version.

borne-out *in vivo* (Shaffer et al., 2006), as rats and dogs converted **1** to **4** in greater amounts (11% and 63% of total dose in urine, respectively) than humans (8%).

Reaction phenotyping studies employing the recombinant enzymes of the major drug metabolizing human P450s suggest that the formation of **2**, arising from biotransformation of the furanopyridine within **1**, is mediated by CYP2D6, a polymorphically expressed enzyme absent in ca. 7% of Caucasians (Shimizu et al., 2003). Interestingly, subject 2F was an outlier from the other seven subjects in that she had the highest plasma (81%) and urine (81%) levels of **1** and the lowest plasma (0.6%) and urine (3%) levels of **2** (Table 5). Although subjects did not undergo CYP2D6 (or any other) genotyping or phenotyping for this study, the observation of one of eight Caucasian subjects (i.e. 13%) showing disparate (relative to all other volunteers) systemic exposures to **1**, and urinary and plasma quantitative profiles nearly devoid of **2** with higher levels of **1**, correlate with both the identification of CYP2D6 as the only major recombinant CYP consuming **1** (and converting it to **2**) and the demographics of Caucasian CYP2D6 poor metabolizers (PMs). However, if subject 2F was a CYP2D6 PM, the detection of **2** within both her urine and plasma would imply that another oxidative enzyme other than the P450s tested *in vitro* contributes minimally to its formation. Similarly, although CYP2D6 also formed **4** *in vitro*, if subject 2F was truly deficient in CYP2D6 then her similar urinary and circulatory quantities of **4** versus the other seven volunteers suggests *N*-oxide formation in humans may be regulated more so by renal FMO1 (with possibly extremely minimal contributions by hepatic FMO3), which readily converted **1** to **4** *in vitro*. Albeit eight Caucasian subjects is an inadequate sampling size for assessment of the impact of a genetic polymorphism, these data do prompt speculation that subject 2F

indeed lacked CYP2D6, and that this isozyme largely mediates the biotransformation of **1** to **2** in humans. This observation should lead to the study of the pharmacokinetics of **1** in CYP2D6 PMs.

Acknowledgments

The authors would like to acknowledge: Dr. Brad D. Maxwell and Mr. John Easter for the synthesis and purification of [^{3}H]**1**; Dr. Donn G. Wishka and Ms. Karen M. Yates for the synthesis and purification of **1**, **2** and **4**; Mr. Bruce A. Thornburgh for providing **M5**; Messrs. James P. Sams and Mark G. Johnson for conducting fecal radioanalysis; and, Dr. Emery C. Polasek for medical monitoring.

References

Baillie TA, Cayen MN, Fouda HG, Gerson RJ, Gree JD, Grossman SJ, Klunk LJ, LeBlanc B, Perkins DG and Shipley LA (2002) Drug Metabolites in Safety Testing. *Toxicol Appl Pharmacol* **182:**188-196.

Breier A (2005) Developing Drugs for Cognitive Impairment in Schizophrenia. *Schizophr Bull* **31:**816-822.

Cashman JR (2004) The implications of polymorphisms in mammalian flavin-containing monooxygenases in drug discovery and development. *Drug Discov Today* **9:**574-581.

Court J, Spurden D, Lloyd S, McKeith I, Ballard C, Cairns N, Kerwin R, Perry R and Perry E (1999) Neuronal Nicotinic Receptors in Dementia with Lewy Bodies and Schizophrenia: α-Bungarotoxin and Nicotine Binding in the Thalamus. *J Neurochem* **73:**1590-1597.

Fisher MB, Yoon K, Vaughn ML, Strelevitz TJ and Foti RS (2002) Flavin-containing Monooxygenase Activity in Hepatocytes and Microsomes: In Vitro Characterization and In Vivo Scaling of Benzydamine Clearance. *Drug Metab Dispos* **30:**1087-1093.

Freedman R, Coon H, Myles-Worsley M, Orr-Urtreger A, Olincy A, Davis A, Polymeropoulos M, Holik J, Hopkins J, Hoff M, Rosenthal J, Waldo MC, Reimherr F, Wender P, Yaw J, Young DA, Breese CR, Adams C, Patterson D, Adler LE, Kruglyak L, Leonard S and Byerley W (1997) Linkage of a neurophysiological deficit in schizophrenia to a chromosome 15 locus. *Proc Natl Acad Sci USA* **94:**587-592.

Green MF and Braff DL (2001) Translating the basic and clinical cognitive neuroscience of schizophrenia to drug development and clinical trials of antipsychotic medications. *Biol Psychiatry* **49:**374-384.

Hajos M, Hurst RS, Hoffman WE, Krause M, Wall TM, Higdon NR and Groppi VE (2005) The Selective a7 Nicotinic Acetylcholine Receptor Agonist PNU-282987 [*N*-[(*3R*)-1-Azabicyclo[2.2.2]oct-3-yl]-4-chlorobenzamide Hydrochloride] Enhances GABAergic Synaptic Activity in Brain Slices and Restores Auditory Gating Deficits in Anesthetized Rats. *J Pharmacol Exp Ther* **312:**1213-1222.

Hamilton RA, Garnett WR and Kline BJ (1981) Determination of Mean Valproic Acid Serum Levels by Assay of a Single Pooled Sample. *Clin Pharmacol Ther* **29:**408-413.

Holden C (2003) Deconstructing Schizophrenia. *Science (Wash DC)* **299:**333-335.

Kitagawa H, Takenouchi T, Azuma R, Wesnes KA, Kramer WG, Clody DE and Burnett AL (2003) Safety, Pharmacokinetics, and Effects on Cognitive Function of Multiple Doses of GTS-21 in Healthy, Male Volunteers. *Neuropsychopharmacology* **28:**542-551.

Lemoine A, Johann M and Cresteil T (1990) Evidence for the Presence of Distinct Flavin-Containing Monooxygenases in Human Tissues. *Arch Biochem Biophys* **276:**336-342.

Marutle A, Zhang X, Court J, Piggott M, Johnson M, Perry R, Perry E and Nordberg A (2001) Laminar distribution of nicotinic receptor subtypes in cortical regions in schizophrenia. *J Chem Neuroanat* **22:**115-126.

Maxwell BD, Wishka DG, Yates KM and Rogers BN (2006) Preparation of [^{3}H]PHA-543613, an Agonist of the α7 Nicotinic Acetylcholine Receptor, and Observation of a Unique 1,4-Shifted Tritiated Product. *J Labelled Compd Radiopharm* **submitted**.

Meltzer HY and McGurk SR (1999) The effects of clozapine, risperidone and olanzapine on cognitive function in schizophrenia. *Schizophr Bull* **25:**233-255.

Obach RS, Baxter JG, Liston TE, Silber BM, Jones BC, MacIntyre F, Rance DJ and Wastall P (1997) The Prediction of Human Pharmacokinetic Parameters from Preclinicaland In Vitro Metabolism Data. *J Pharmacol Exp Ther* **283:**46-58.

Olincy A, Harris JG, Johnson LL, Pender V, Kongs S, Allensworth D, Ellis J, Zerbe GO, Leonard S, Stevens KE, Stevens JO, Martin L, Adler LE, Soti F, Kem WR and Freedman R (2006) Proof-of-Concept Trial of an α7 Nicotinic Agonist in Schizophrenia. *Arch Gen Psychiatry* **63:**630-638.

Rettie AE and Fisher MB (1999) Transformation Enzymes: Oxidative; Non-P450, in: *Handbook of Drug Metabolism* (Woolf TF ed), Marcel Dekker, Inc., New York.

Sawa A and Snyder SH (2002) Schizophrenia: Diverse Approaches to a Complex Disease. *Science (Wash DC)* **296:**692-695.

Shaffer CL, Gunduz M, Thornburgh BA and Fate GD (2006) Using a Tritiated Compound to Elucidate Its Preclinical Metabolic and Excretory Pathways In Vivo: Exploring Tritium Exchange Risk. *Drug Metab Dispos* **34:**1615-1623.

Shimizu T, Ochiai H, Asell F, Shimizu H, Saitoh R, Hama Y, Katada J, Hashimoto M, Matsui H, Taki K, Kaminuma T, Yamamoto M, Aida Y, Ohashi A and Ozawa N (2003) Bioinformatics Research on Inter-racial Difference in Drug Metabolism I.

Analysis on Frequencies of Mutant Alleles and Poor Metabolizers on CYP2D6 and CYP2C19. *Drug Metab Pharmacokinet* **18:**48-70.

Smith DA and Obach RS (2005) Seeing Through the MIST: Abundance Versus Percentage. Commentary on *Metabolites In Safety Testing*. *Drug Metab Dispos* **33:**1409-1417.

Stevens KE, Kem WR, Mahnir VM and Freedman R (1998) Selective α_7-nicotinic agonists normalize inhibition of auditory response in DBA mice. *Psychopharmacology* **136:**320-327.

Wishka DG, Walker DP, Yates KM, Reitz SC, Jia S, Myers JK, Olson KL, Jacobson EJ, Wolfe ML, Groppi VE, Hanchar AJ, Thornburgh BA, Cortes-Burgos LA, Wong E, Staton BA, Raub TJ, Higdon NR, Wall TM, Hurst RS, Walters RR, Hoffman WE, Hajos M, Franklin S, Carey G, Gold LH, Cook KK, Sands SB, Zhao SX, Soglia JR, Kalgutkar AS, Arneric SP and Rogers BN (2006) Discovery of PHA-543,613, an Agonist of the α7 Nicotinic Acetylcholine Receptor, for the Treatment of Cognitive Deficits in Schizophrenia: Synthesis and SAR. *J Med Chem* **49:**4425-4436.

Footnote

M.G. current address: Novartis Institutes for BioMedical Research, Department of Metabolism and Pharmacokinetics, 250 Massachusetts Ave., Cambridge, MA 02139

Legends for Figures

Figure 1. Chemical structure of protonated [^{3}H]**1** (*m/z* 272) and its collision-induced dissociation fragmentation pathway.

Figure 2. Semilogarithmic (top) and linear (bottom) plots of mean plasma concentrations of **1** (filled symbols) and total radioactivity (unfilled symbols) in females (♦) and males (▲). Concentrations of **1** and total radioactivity were determined from non-lyophilized and lyophilized plasma, respectively.

Figure 3. Enzyme kinetics of the oxidation of **1** to **2** (◊) and **4** (□) in recombinant human CYP2D6. Each data point is an average of two incubations.

Figure 4. An overview of the proposed metabolic pathways of **1** in humans. Bold numerical designations are for observed metabolites; all other structures are putative metabolite intermediates. [O], enzyme-mediated oxidation; H_2, enzyme-mediated reduction.

Tables

Table 1. Human volunteer demographic data and radioactive dose

Subject[a]	Age (y)	Weight (kg)	BMI (kg/m^2)	Dose (μCi)
1F	31	71.7	30.4	163.2
2F	46	60.3	23.2	163.3
3F	41	60.8	22.3	163.2
4F	51	80.5	29.5	163.3
11M	35	83.5	27.7	163.2
12M	28	73.5	22.9	163.2
13M	24	78.5	24.8	163.3
14M	23	64.9	21.1	163.3
Mean ± SD	35 ± 10	71.7 ± 9.0	25.2 ± 3.5	163.3 ± 0.1

[a]F and M denote female and male volunteer, respectively.

DMD Fast Forward. Published on April 19, 2007 as DOI: 10.1124/dmd.106.014449
This article has not been copyedited and formatted. The final version may differ from this version.

Table 2. Mass recoveries (% of dose) and excretory routes in humans after a single 40 mg oral dose of [^{3}H]**1**

	Urine	Feces	Total
Female	107 ± 5	1.4 ± 0.1	108 ± 5
Male	106 ± 7	1.9 ± 0.3	108 ± 7

Table 3. Mean gender pharmacokinetics of **1** and total radioactivity in humans after a single 40 mg oral dose of [^{3}H]**1**

	1		Total Radioactivity[a]	
	Female	Male	Female	Male
T_{max} (h)	1.50 ± 0.41	1.25 ± 0.65	1.81 ± 0.75	1.63 ± 0.63
C_{max}[b]	212 ± 30	151 ± 29	401 ± 59	337 ± 77
$t_{1/2}$ (h)	11.8 ± 3.7	8.78 ± 0.95	13.0 ± 5.4	9.02 ± 2.94
$AUC_{0-tlast}$[c,d]	3040 ± 1310	1770 ± 220	4100 ± 600	2960 ± 460
AUC_{0-12}[c]	1630 ± 310	1140 ± 170	3130 ± 320	2470 ± 350
CL_p/F (mL/min/kg)	3.72 ± 1.46	5.08 ± 0.48	na	na
CL_R/F[e] (mL/min/kg)	2.28 ± 0.56	3.59 ± 0.23	na	na
$(CL_R/F)/(f_u \bullet GFR)$[f]	1.6 ± 0.4	2.8 ± 0.4	na	na

na: not applicable.

[a]Determined from lyophilized plasma.

[b]Units are ng/mL and ng-eq./mL for **1** and total radioactivity, respectively.

[c]Units are ng•h/mL and ng-eq.•h/mL for **1** and total radioactivity, respectively.

[d]T_{last} was 48 h for **1** and 16 h for total radioactivity.

[e]Calculated by Ae_{0-48}/AUC_{0-48} and subject weight-normalized.

[f]Plasma free fraction (f_u) was 0.81, GFR was 120 mL/min and subject weight-normalized.

DMD Fast Forward. Published on April 19, 2007 as DOI: 10.1124/dmd.106.014449
This article has not been copyedited and formatted. The final version may differ from this version.

Table 4. Chromatographic and mass spectral data for **1** and its human metabolites

Compound	LC t_R (min)	$[M+H]^+$ (*m/z*)	CID-generated Fragments[a] (*m/z*)
1	23.3	272	163, 146, 118, **110**, 82
2	18.4	306	288, 262, 180, 162, 152, 127, **110**, 82
4	23.5	288	164, 146, 118, **109**, 82
M5	22.1	448	412, 314, **272**, 163, 110

[a]Bold font denotes base peak *m/z* within CID spectrum.

Table 5. Individual excretory and circulatory metabolite profiles in humans after a single 40 mg oral dose of [^{3}H]**1**

	Urine[a]									
	Female					Male				
Compound	1F	2F	3F	4F	Mean ± SD	11M	12M	13M	14M	Mean ± SD
1	67.3	81.1	48.0	62.6	64.8 ± 13.7	73.8	77.3	69.0	65.9	71.5 ± 5.0
2	29.8	3.1	45.3	26.1	26.1 ± 17.4	20.9	23.0	19.9	35.3	24.8 ± 7.1
4	7.8	8.1	10.1	8.0	8.5 ± 1.1	6.9	8.2	5.3	7.3	6.9 ± 1.2
M5	2.9	2.9	1.9	1.9	2.4 ± 0.6	2.2	1.2	1.0	1.3	1.4 ± 0.6
^{3}H Profiled (%)[b]	96.3	95.2	95.7	93.9	95.3 ± 1.0	97.9	98.0	98.9	99.0	98.5 ± 0.6
	Plasma[c]									
	Female					Male				
Compound	1F	2F	3F	4F	Mean ± SD	11M	12M	13M	14M	Mean ± SD
1	63.6	80.6	40.7	59.0	61.0 ± 16.4	61.5	65.7	53.3	47.4	57.0 ± 8.2
2	23.8	0.6	41.4	21.6	21.8 ± 16.7	22.3	18.4	29.9	25.4	24.0 ± 4.9
4	0.9	4.2	4.7	5.4	3.8 ± 2.0	4.7	2.3	5.5	4.4	4.2 ± 1.4
M5	4.6	4.3	4.9	4.4	4.5 ± 0.3	3.8	1.7	3.0	1.8	2.6 ± 1.0
^{3}H Profiled (%)	92.9	89.7	91.7	90.4	91.1 ± 1.5	92.3	88.1	91.7	79.0	87.7 ± 6.2

[a]% of dose.

[b]% of total dose excreted in urine profiled.

[c]% of total ^{3}H $AUC_{0–12}$ profiled.

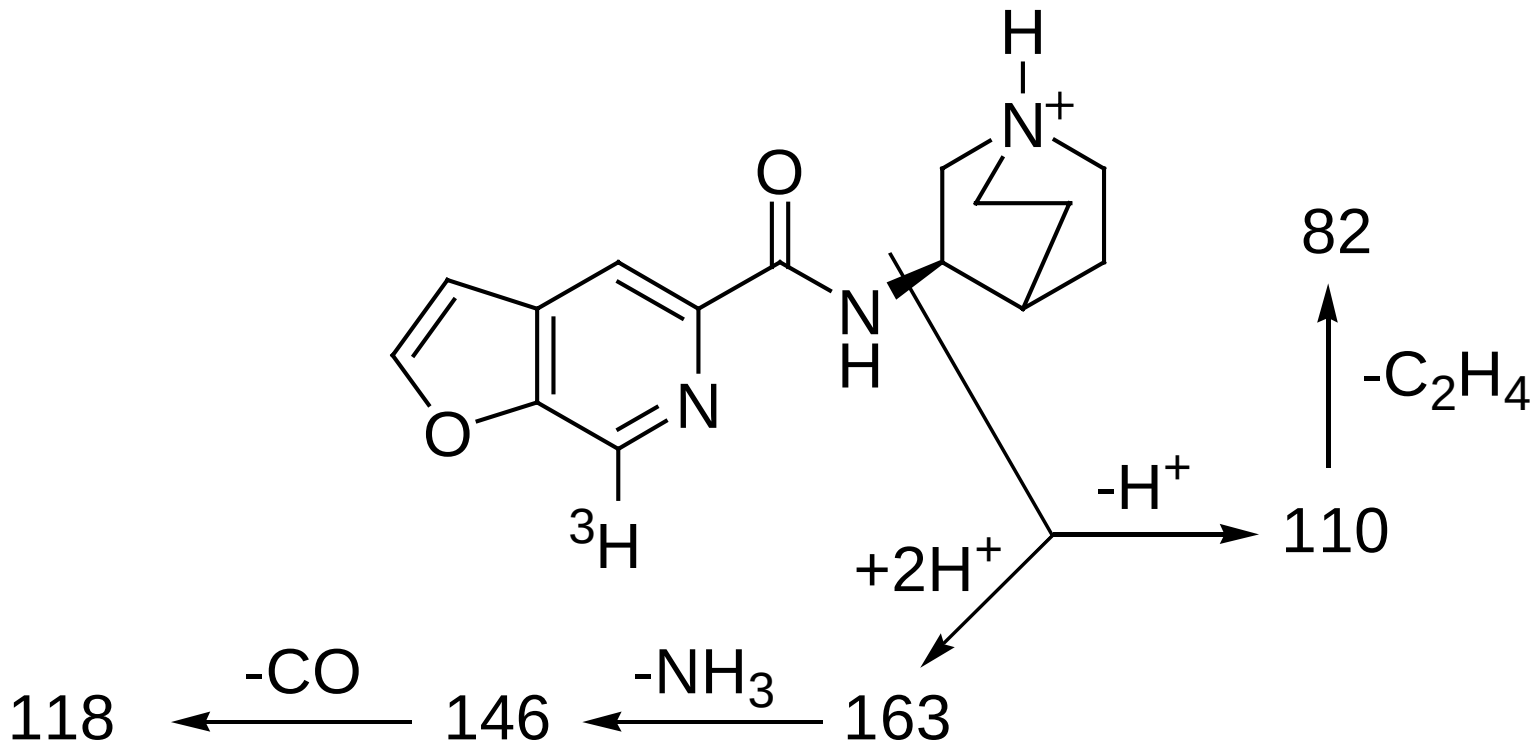

Figure 1

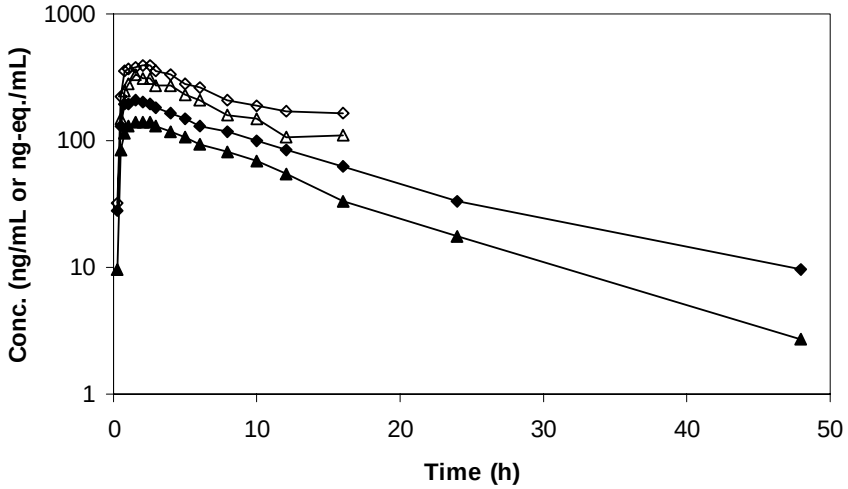

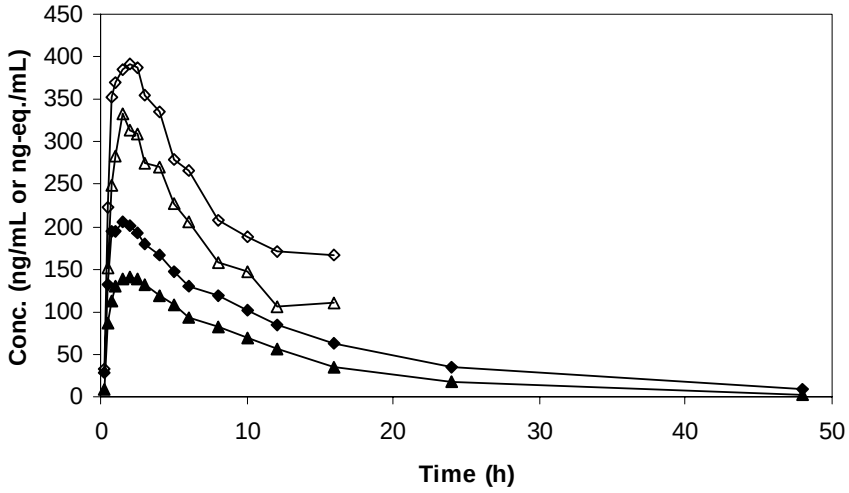

Figure 2

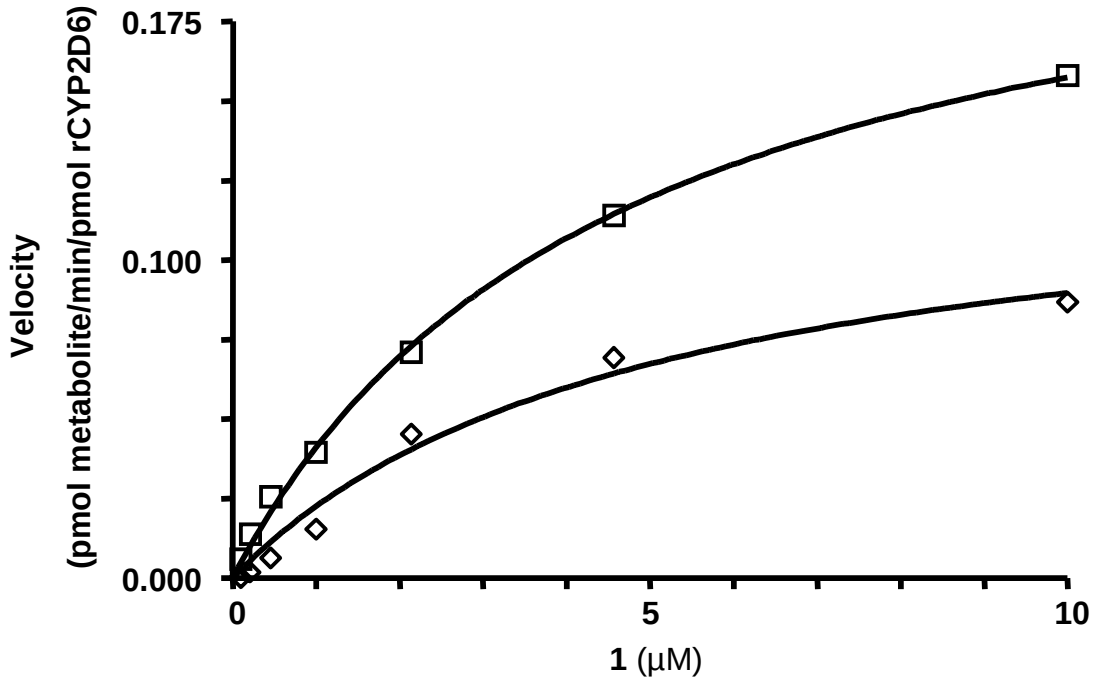

Figure 3

DMD Fast Forward. Published on April 19, 2007 as DOI: 10.1124/dmd.106.014449
This article has not been copyedited and formatted. The final version may differ from this version.

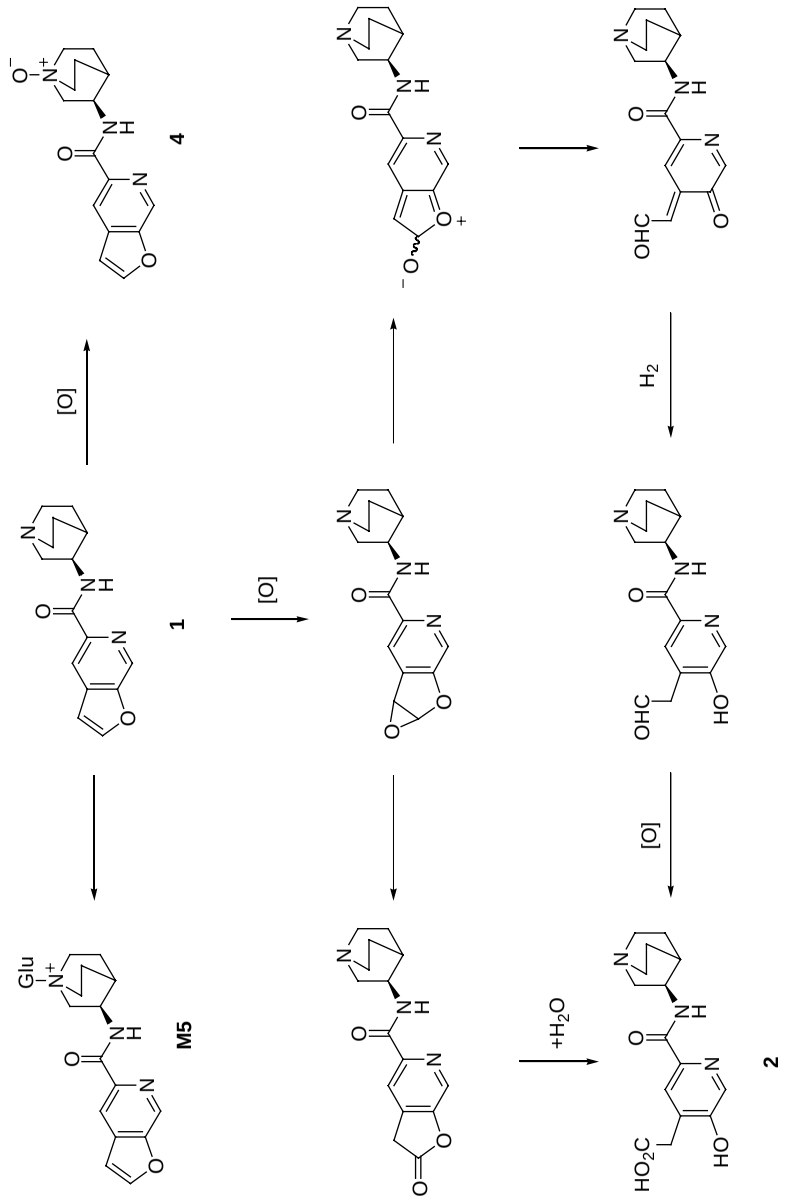

Figure 4